

# A Resource Allocation Method for Achieving Optimal Reliability in a Lunar Architecture

David A. Young\* and Dr. Alan Wilhite†

*Space Systems Design Lab  
Guggenheim School of Aerospace Engineering  
Georgia Institute of Technology, Atlanta, GA, 30332-0150  
David.Young@gatech.edu*

In January 2005, President Bush announced the Vision for Space Exploration. This vision involved a progressive expansion of human capabilities beyond Low Earth Orbit beginning with a return to the moon starting no later than 2020. Current design processes utilized to meet this vision employ performance based trade studies to determine the lowest cost, highest reliability solution. In these design processes, designers trade independent performance variables and then calculate the design discriminators, reliability and costs, of the different architectures. The methodology implemented in this paper focuses on a concurrent evaluation of the performance, cost, and reliabilities of lunar architectures. This process directly addresses the top level requirements early in the design process and allows the decision maker to evaluate the highest reliability, lowest cost lunar architectures without being distracted by the performance details of the architecture.

To achieve this methodology of bringing optimal cost and reliability solutions to the decision maker, parametric performance, cost, and reliability models are created to model each vehicle element. These models were combined using multidisciplinary optimization techniques and response surface equations to create parametric vehicle models which quickly evaluate the performance, reliability, and cost of the vehicles. These parametric models, known as ROSETTA models, combined with a life cycle cost calculator provide the tools necessary to create a lunar architecture simulation. The integration of the tools into an integrated framework that can quickly and accurately evaluate the lunar architectures is presented. This lunar architecture selection tool is verified and validated against the Apollo lunar architectures. The results of this lunar architecture selection tool are then combined into a Pareto frontier to guide the decision maker to producing the highest reliability architecture for a given life cycle cost.

The advantages of this method over traditional design processes are numerous. With this presented methodology, the decision maker can transparently choose a lunar architecture solution based upon the high level design discriminators. This method can achieve significant reductions in life cycle costs keeping the same architecture reliability as a traditional design process point solution. This methodology also allows the decision maker to choose a solution which achieves a significant reduction in failure rate while maintaining the same life cycle costs as the point solution of a traditional design process.

## Nomenclature

<i>Al</i>	=	Aluminum
<i>Al-Li</i>	=	Aluminum-Lithium
<i>ATLAS</i>	=	Advanced Technology and Lifecycle Analysis System
<i>CER</i>	=	Cost Estimating Relationships
<i>CH4</i>	=	Methane
<i>CM</i>	=	Command Module

---

\*Graduate Research Assistant, School of Aerospace Engineering, Student member AIAA.

† NASA Langley Professor in Advanced Aerospace Systems Architecture, School of Aerospace Engineering, Associate Fellow AIAA.

<i>DDT&amp;E</i>	= Design, Development, Testing, and Evaluation
<i>DSM</i>	= Design Structure Matrices
<i>EOR</i>	= Earth Orbit Rendezvous
<i>FTA</i>	= Fault Tree Analysis
<i>Gr-Ep</i>	= Graphite Epoxy
$I_{sp}$	= Specific Impulse
<i>LH2</i>	= Liquid Hydrogen
<i>LLO</i>	= Low Lunar Orbit
<i>LM</i>	= Lunar Module
<i>LOC</i>	= Loss of Crew
<i>LOR</i>	= Lunar Orbit Rendezvous
<i>LOX</i>	= Liquid Oxygen
<i>MER</i>	= Mass Estimating Relationship
<i>MMC</i>	= Metal Matrix Composites
<i>N2O4</i>	= Nitrogen Tetroxide
<i>NAFCOM</i>	= NASA Air Force Cost Model
<i>ROSETTA</i>	= Reduced Order Simulation for Evaluating Technologies and Transportation Architecture
<i>RPI</i>	= Refined Petroleum-1
<i>RSM</i>	= Response Surface Methodology
<i>SM</i>	= Service Module
<i>SSDL</i>	= Space Systems Design Laboratory
<i>STS</i>	= Space Transportation System
<i>TFU</i>	= Theoretical First Unit
<i>Ti</i>	= Titanium
<i>UDMH</i>	= Unsymmetrical Dimethylhydrazine

## I. Introduction

The purpose of this research is to improve on the design practices currently employed by the aerospace community. Currently top level design discriminators, such as cost and reliability, are calculated after the vehicle configurations are set. These discriminators are then used to select the winning design among the different candidate designs. This research proposes a methodology to pull these important design discriminators to the front of the design process by combining physics-based parametric models with multidisciplinary optimization techniques and Pareto frontiers to visualize the ideal reliability and cost architecture solutions.

There is a significant amount of research in the operations management community about the need for the decision maker to be provided with not only the optimal solution for the requirements, but also the optimal points for the off nominal requirements. This is especially true in spacecraft design, where life cycle costs can be in the billions of dollars and programs last for decades. The long and costly programs are subject to the whims of the public and funding can either increase or decrease depending on the decision maker leading the project at the time. Because of this instability it is important to have an understanding of the entire design space so that decisions can be made which will be robust to changing project budgets.

Although optimal engineering solutions can be found for a given set of requirements, organizational inertia can push these new techniques aside in favor of old less efficient ways. The complications of applying new design techniques to industry are addressed in the literature [1, 2, 3]. As these references demonstrate adoption of a new method, especially a non-transparent method is very difficult regardless of the benefit offered. Because of this non-acceptance, the method proposed in this paper attempts to address these issues by adapting conventional conceptual design tools into parametric design models through response surface equations. This method also increases the transparency of the process by providing the decision maker with the entire set of solutions in the form of a Pareto frontier. This frontier of optimal solutions allows the decision maker to choose the optimal solution from the best data available and does not attempt to hand the decision maker a solution which he/she has not chosen. This allows the decision maker to be invested in the solution to the architecture while avoiding non-optimal configurations.

## II. Methodology

To evaluate the performance, cost, and reliability of a lunar architecture concurrently, it is necessary to create parametric models of the vehicle elements that make up the lunar architecture. These parametric tools can then be evaluated in the architecture to create the total architecture cost and reliability. This can then be used to compare the different architecture configurations and lunar modes. A Reduced Order Simulation for Evaluating Technologies and Transportation Architecture (ROSETTA) model is a parametric design tool utilized by the Space System Design Laboratory at the Georgia Institute of Technology to quickly evaluate how changing the design variable affects a vehicle. A ROSETTA model is a spreadsheet model that uses Response Surface Methodology (RSM) to approximate each of the design disciplines described [4]. The ROSETTA model can also be used to calculate the viability of a vehicle if the DDT&E, operations costs, and economics of the vehicle are included in the model.

### A. Performance

To calculate the performance of the lunar architecture it is necessary to calculate the resulting performance of all of the vehicle elements of the architecture. To calculate this vehicle performance, a ROSETTA model is created for each vehicle. The Lunar Module ROSETTA model is given as an example to demonstrate the procedure to be followed in the creation of a ROSETTA model. The Design Structure Matrix (DSM) for the ROSETTA Lunar Module is given below as Figure 1.

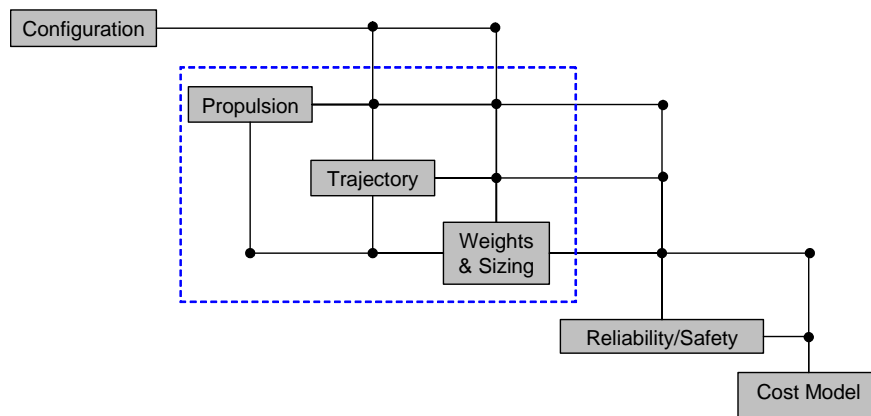


**Figure 1: Design Structure Matrix for ROSETTA Lunar Module.**

As this DSM demonstrates, there are four separate disciplines are integrated to calculate the performance characteristics of the Lunar Module. As with most ROSETTA models, there is a strong coupling between the propulsion, trajectory and weights disciplines. This coupling is addressed in the ROSETTA model through iteration in the Excel spreadsheet. This iteration automatically occurs until the inputs to the different CAs are all consistent. This represents a closed vehicle solution.

A lunar module, as defined in this ROSETTA model, must be capable of transporting humans and/or cargo to and from the lunar surface. The vehicles must also be able to support changing payload weights as the weights of the other vehicles in the mission change. To facilitate these different mission requirements, the ROSETTA model was setup to parametrically scale based upon changing mission requirements. A summary of the ranges of mission requirements that are defined by the ranges of the individual ROSETTA models is given as Table 1.

**Table 1: Mission Parameters Ranges for ROSETTA Lunar Module.**

<i>Mission Ranges</i>	<i>Minimum</i>	<i>Maximum</i>
Crew Number	0	6
Payload to LS	500 kg	50,000 kg
Payload to LLO	100 kg	50,000 kg
Payload for LOI Burn	0 kg	50,000 kg
Mission time	3 days	14 days
On Orbit Delay	0 days	180 days
Number of Stages	1	2

This table gives the mission specific parameters that the ROSETTA model is able to accommodate. There are also over 50 other performance based configuration inputs that the vehicle model uses to simulate a multitude of different lunar landers. These configuration parameters have a large effect on the performance of the vehicle. A summary of some of the most important configuration parameters is provided as Table 2.

**Table 2: Configuration Inputs for ROSETTA Lunar Module.**

<i>Structural Types</i>	<i>Propellant Types</i>	<i>Engine Cycle Types</i>
Aluminum	LOX/LH2	Pressure Fed
Aluminum-Lithium	UDMH/N2O4	Expander
Titanium	LOX/CH4	
Graphite Epoxy		
Metal Matrix Composite		

The mission parameters (Table 1) and the configuration inputs (Table 2) are treated as inputs to the design structure matrix and define the configuration for the ROSETTA Lunar Module.

The propulsion discipline involves a Response Surface Equation (RSE) of REDTOP 2 engine performance conceptual design tool [5]. Each propellant combination and cycle type requires a different RSE. These RSEs require the propellant type, cycle type, thrust level, chamber pressure, and O/F ratio as inputs. The model then calculates the resulting  $I_{sp}$  and engine T/W to the ROSETTA model [6]. This  $I_{sp}$  and T/W are then passed to the trajectories and weights disciplines.

The trajectory discipline involves a RSE of Program to Optimize Simulated Trajectories (POST 3D) [7]. This program is an industry standard three degrees of freedom trajectory simulator that optimizes the weight consumed in a trajectory. The RSE of the POST simulation requires the total vehicle stage weight from the weights analysis and the thrust and  $I_{sp}$  from the propulsion analysis [8]. The resulting  $\Delta V$  for the trajectories are then passed to the weights analysis to calculate the total propellant required and the tank sizes.

The weights and sizing discipline uses a series of industry standard Mass Estimating Relationships (MERs) to approximate the vehicle weights [9]. These MERs combined with semi-empirical tank sizing relationships to calculate the size of the tanks necessary to hold the propellant [10]. The structural strengths and densities of the material types are defined from the Humble [11]. This propellant mass is calculated with the trajectory  $\Delta V$  and  $I_{sp}$  from rocket equation.

$$\Delta V_{Traj} = g_0 I_{sp} LN \left( \frac{M_{Propellant} + M_{Inert}}{M_{Inert}} \right) \quad (1)$$

Where:  $g_0$  is the gravitational constant  
 $M_{propellant}$  is the propellant mass  
 $M_{inert}$  is the inert mass of the vehicle

The calculated propellant mass is then combined with other MERs to produce the total vehicle mass of the system. This vehicle mass is then iterated with the propulsion (via thrust and T/W ratios) and trajectory to close the lunar module vehicle design. The Excel implementation of the ROSETTA model allows the vehicle's performance to be calculated quickly and is portable to any computer operating Microsoft Office. The resulting mass estimations for the vehicle weight can then be passed to the other ROSETTA models of the lunar architecture.

## **B. Reliability and Safety**

To model the reliability and safety disciplines in the ROSETTA model, a new approach was needed. Traditionally, fault trees are used to calculate the reliability of a system based upon each assumed subsystem reliability. This static approach is generally sufficient for calculating the reliability of a system and has been used for all types of systems, including the Space Shuttle. Unfortunately, the FTA analysis is not sufficient to calculate the reliabilities of changing vehicle configurations since it requires that the number and placement of the subsystems be static to calculate the total reliability of the system. For this methodology, it is imperative that the fault trees change dynamically to adjust to the changing vehicle configurations, such as number of engines, propellant types, etc. To accomplish this dynamically changing fault tree, a mathematical representation of the fault tree was created in Excel and was allowed to change based upon the input vehicle configurations. These dynamically changing fault trees will be implemented in every ROSETTA model to accurately calculate the resulting vehicle reliability based upon the changing configurations.

These dynamically changing fault trees must be able to not only calculate the loss of mission reliability of a vehicle but also the loss of crew safety. These calculations differ by the severity of the failure and the ability of the crew to survive the failure type. For most instances, the difference between the types of failures will depend on the vehicle and the subsystem which failed. For most models, the difference between LOM and LOC will be established via a percentage of subsystem failures that result in a LOC event. Even if a LOC event occurs, it does not necessarily result in a loss of crew. Some vehicles have emergency abort systems that will save the crew in the event of a LOC event occurs. The success of these systems is still subject to the reliability of the crew abort system. For vehicles with such an abort system, the LOC number is inflated by the reliability of that abort system via a parallel reliability calculation.

The dynamic fault tree analysis integrated into this methodology requires that the individual subsystem reliabilities be defined and input into the base of the fault tree. These individual subsystem reliabilities are generally considered to be inputs into the vehicle fault tree. In the case of a propulsion subsystem, the subsystem reliabilities are highly dependant on the configuration of the vehicle. The individual element reliabilities can be found in literature, but models have to be developed to calculate the total subsystem reliability that can be included in the dynamic fault tree analysis.

The propulsion subsystem reliability is a combination of different reliability models combined to account for the possible failure modes of the each subsystem. These reliability models include:

- Common Cause Failure Model
- Catastrophic Engine Failure Model

Each of these models is combined into one branch of the dynamically changing fault tree analysis to provide the overall propulsion system reliability.

Common Cause Failure (CCF) is a reliability technique that attempts to model the failures that are inherent due to flaws in all redundant systems in an element. A standard definition of common cause failure is, "A subset of dependent events in which two or more component fault states exist at the same time, or in a short interval, and are direct result of a shared cause." [12]. These CCFs usually occur in systems where multiple, usually redundant, components all share the same flaw. This flaw can be a manufacturing, software, or other problem that is common to all redundant systems in an element. An example of a CCF is a flaw in the materials properties found in many propellant tanks, which cause all tanks in a system to fail when stressed. In this case a redundant system, such as multiple tanks of a fuel cell in a power system, can fail simultaneously due to a materials flaw in the construction of many propellant tanks.

There are many proposed methods to model CCF. These methods include both explicit and implicit methods of modeling a CCF [13]. An explicit method treats the common cause as a separate event in the fault tree analysis. An implicit method treats the common cause failure as an algebraic unreliability expression, which is then included in the reliability calculation input into the fault tree analysis. In this methodology an explicit method is chosen for extensibility because it is generally difficult to derive an algebraic expression of system unreliability [14].

There are many different explicit methods that can be chosen to model common cause failures in a dynamic fault tree analysis. In this methodology a single parameter or  $\beta$  model will be used [15]. A single parameter model is a model that uses a single  $\beta$  parameter in parallel with the redundant components in a subsystem. This  $\beta$  parameter is defined as a combination of independent failure rates and common cause failure rates as given by equation 2.

$$\beta = \frac{\lambda_c}{\lambda_c + \lambda_I} \quad (2)$$

Where:  $\lambda_c$ =failure rate due to common cause failures  
 $\lambda_I$ =failure rate due to independent failures

This single parameter model is explicit and is therefore treated as an independent event in series with the component failure rate in the fault tree analysis.

Common cause failures are not the only specific breakdown of the subsystem system reliability used in this methodology. Failure rates are broken down in this research according to the four types of failures defined in Huang et al. [16]. This breakdown divides failure rates into four categories:

- Catastrophic Failures
- Non-Catastrophic Failures
- Preventable Catastrophic Failures
- Unnecessary Shutdown Failures

A catastrophic failure is defined as an uncontained failure the immediately results in a loss of vehicle. This, in turn, will result in a loss of crew unless a crew abort system is in place. Historically, catastrophic failure rates for engines range between 20% and 40% [16]. This catastrophic failure rate was generally derived for propulsion subsystems but is generalized for all subsystems.

Non-catastrophic failure rates are considered failures that are contained by the failing element. An example of this is a failure that causes the system to shutdown, but the vehicle can still operate with a redundant system. The aforementioned shuttle main engine cutoff sensors are an example of a non-catastrophic failure. If the sensor fails “wet,” or the engine shuts down when fuel is still present, the failure is contained to this subsystem. Since the ECO sensors have redundancy, this failure would not result in a loss of mission.

The third type of failure is the preventable catastrophic failure. This type of failure would result in a catastrophic failure if the safety systems did not shut down the operating equipment. An example of this would be an engine health management system shutting down an engine when redlines are exceeded. If the health management system was not present, a catastrophic failure would have occurred; but it was prevented by the safety system.

The fourth and final type of failure is unnecessary shutdown failures. These failures are a result of the safety systems sensor failure, where the operating element is shut down when no real failure has occurred. This can be found in almost any avionics or health management system where redlines are too restrictive.

Each of these types of failures is represented as basic events in the fault tree analysis. These failure rates can then be combined with the common cause failure rate to produce an entire subsystem failure rate. A representation of what a propulsion system fault tree would look like with the CCF and catastrophic engine failure rates are included is shown as Figure 2.

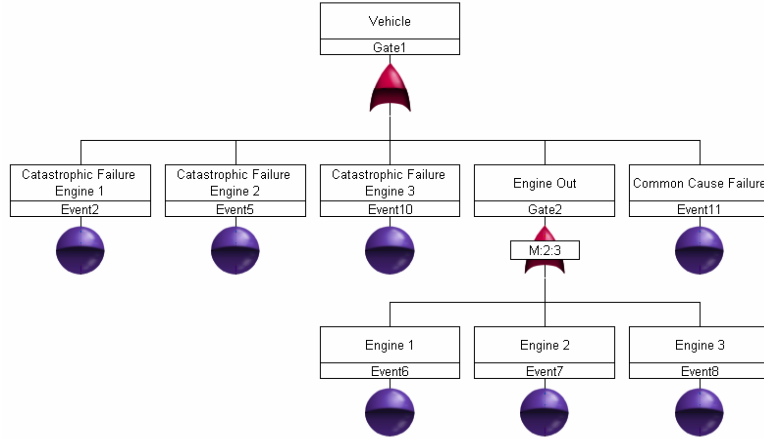


**Figure 2: Fault Tree Representation of the Propulsion System for a Generic Launch Vehicle Using Relex [17].**

This figure shows a three engine propulsion system with engine out vehicle configuration represented as fault tree. As this figure shows the catastrophic failure fraction rate for each engine must be treated as an independent event. A catastrophic failure of any of the engines causes a failure of the entire vehicle. Common cause failure is also treated much like a catastrophic failure rate in that it is an independent event which is in series with the actual elements of the vehicle. The engine out system is treated as a k out of n system. It should be noted that although the k out of n system increases the reliability, the addition of an extra engine catastrophic rate decreases the reliability over an ideal k out of n system.

To complete a dynamic fault tree analysis this fault tree must be mathematically described in the ROSETTA model. To mathematically model this reliability, a catastrophic engine failure fraction was added to a k out of n system. The mathematical model derived from Huang et al. is given [16]:

$$R_{PS} = [1 - (C_F(1 - R_T) + P_F(1 - R_T) + U_F(1 - R_T) + NCF_F(1 - R_T))]^N \quad (3)$$

$$R_{PS(EO)} = (1 - C_F(1 - R_T))^N [(1 - (1 - C_F)(1 - R_T))^N + N(1 - (1 - C_F)(1 - R_T))^{N-1} (1 - C_F)(1 - R_T)] \quad (4)$$

Where:  $R_{PS}$  is the reliability of the propulsion system

$R_{PS(EO)}$  is the reliability of the propulsion system with engine out

$C_F$  is the catastrophic failure rate

$R_T$  is the single engine reliability

$P_F$  is the preventable failure fraction

$U_F$  is the unnecessary shutdown failure fraction

$NCF_F$  is the non-catastrophic failure fraction

$N$  is the number of engines

This model for loss of mission reliability can be extended to calculate the loss of crew reliability. The loss of crew number includes a factor to account for the fact that the crew may survive a non-catastrophic failure. That factor is included as a vehicle stage specific percentage of the trajectory where the crew can successfully survive a non-catastrophic failure. These loss of mission and loss of crew systems representations can be combined with the common cause failure rate to calculate a total loss of mission and loss of crew expression. A summary of the analytical equations for the loss of mission and loss of crew reliabilities follow:

Loss of Mission Reliability:

$$R_{PS} = [1 - (C_F(1 - R_T) + CCF(1 - R_T) + P_F(1 - R_T) + U_F(1 - R_T) + NCF_F(1 - R_T))]^N \quad (5)$$

$$R_{PS(EO)} = (1 - C_F(1 - R_T))^N [(1 - (1 - C_F - \beta)(1 - R_T))^N + N(1 - (1 - C_F - \beta)(1 - R_T))^{N-1} (1 - C_F - \beta)(1 - R_T)] (1 - \beta^*(1 - R_T)) \quad (6)$$

Loss of Crew Safety:

$$R_{PS} = [1 - (C_F(1 - R_T) + CCF(1 - R_T) + [P_F(1 - R_T) + U_F(1 - R_T) + NCF_F(1 - R_T)] * (1 - \%T))]^N \quad (7)$$

$$R_{PS(EO)} = (1 - C_F(1 - R_T))^N [(1 - (1 - C_F - \beta)(1 - R_T)(1 - \%T))^N + N(1 - (1 - C_F - \beta)(1 - R_T)(1 - \%T))^{N-1} (1 - C_F - \beta)(1 - R_T)(1 - \%T)] (1 - \beta^*(1 - R_T)) \quad (8)$$

Where:  $\beta$  is the common cause failure percentage

$\%T$  is the percentage of the trajectory where the crew can survive a non catastrophic failure without a crew escape system

$R_{PS}$  is the reliability of the propulsion system

$R_{PS(EO)}$  is the reliability of the propulsion system with engine out

These equations are implemented in the ROSETTA models to address the subsystem reliabilities that are compiled in the development of the dynamically changing fault tree analysis.

### C. Cost Estimation

To calculate the top level design discriminators, it is necessary to get an accurate cost model to predict the vehicle costs and compile architecture life cycle costs. These CERs are weight based costing relationships that are based upon analogous systems to calculate the Design, Development, Testing, and Evaluation (DDT&E) costs as well as the Theoretical First Unit (TFU) costs. These costs will then be compiled into a Life Cycle Cost (LCC) which will then be combined with the vehicle reliability to calculate the Pareto frontier which will be used to make the lunar architecture mode decision. The cost model used in the ROSETTA models is NAFCOM CER based. The a and b terms are derived from analogous vehicles which can be obtained from NAFCOM 04 for all of the Apollo vehicles [18]. These subsystem based costs are then compiled into a stage cost. This stage cost is then multiplied by NAFCOM relationships for Program Management, Integration, Assembly and Checkout, System Test Operations, Ground Support Equipment, and System Engineering and Integration. A cost margin of 20% is also applied to all vehicles which do not currently exist. The complexity factors for the CERs are all baselined at one and manipulated via the vehicle configuration choices and the cost penalties for using off-nominal reliabilities. These CERs are then linked with the weights calculation page in the ROSETTA models so that as the vehicle scales the costs automatically recalculate.

The complexity factor portion of the CERs is adjusted based upon the vehicle configuration. These complexity factors adjust for the fact that some materials are more expensive per pound than others. An example of this is that a tank made out of Titanium will weigh less than a tank made out of aluminum, but the titanium tank should cost more than the aluminum tank. A summary of the structural complexity factors is given as Table 3 [19].

**Table 3: Complexity Factors for Tank Structural Materials.**

<i>Structure</i>	<i>Complexity Factor</i>
Al	1
Al-Li	1.5
Ti	7
Graphite Epoxy Overwrapped	5
MMC	12

As this table shows, the cost per pound of different spacecraft materials varies greatly. Aluminum is the cheapest and most widely used material. Graphite epoxy is currently estimated to be 5 times the price per pound of Al; however, the actual cost of a tank could be less than that of aluminum because the weight of the tank is significantly lighter due to the higher strength and lower density of graphite epoxy

Once the vehicle costs are calculated for each of the vehicles in the lunar architecture, the total life cycle costs for the architecture can be calculated. The life cycle cost calculator used in this method spreads the DDT&E out over a specified number of years at the beginning of the program. This DDT&E is spread as a Beta function over the specified number of years. Once the DDT&E is paid, a flight rate is assumed and the cost per flight is calculated based upon the production costs for the elements. This learning curve diminishes the cost of subsequent production vehicles because of the knowledge gained in producing the previous vehicle. For this research a learning curve rate of 90% was assumed. The top level inputs to the life cycle cost calculator are:

- Start year for the program
- Total number of years of the program
- Number of years to spread DDT&E
- Flight rate (number of flights per year)
- Learning curve rate

From the top level data and the DDT&E and TFU costs of the different architecture elements, a total life cycle cost can be calculated. The production vehicles decrease in cost via the learning curve rate of 90%. The total LCC is then used along with the loss of mission reliability to calculate the individual points on the Pareto frontier. This generic baseline mission profile (number of years, DDT&E spreading, learning curve, and start year) will be used for all architecture comparisons made in this research.

The life cycle cost described in this methodology does not include an operations cost, nor does it include a disposal cost. The operations cost is highly dependant on the workforce and includes political aspects, both of which are difficult to quantify. The disposal cost is a small percentage of the LCC and is needed for all lunar architectures. Like the Apollo program and soon the space shuttle program, the program elements continue to be utilized long after the vehicle is retired. Because of these reasons the disposal cost is difficult to quantify and will not directly affect the lunar architecture decision.

As with the reliability model described in the previous section, the cost model described above was implemented in the ROSETTA models included in the lunar architecture selection tool. The CERs are implemented in a spreadsheet along with the NAFCOM a and b coefficients to calculate the subsystem DDT&E and TFU costs. The complexity factors for each of the subsystems are calculated as product of the original CER complexity factors calculated from the configuration type and the K-factor calculated from the reliability sheet. Each of these subsystem costs are then compiled to obtain the stage costs for the vehicle. These CERs are then linked with the weights calculated in the performance sections of the ROSETTA model to automatically update the subsystem costs as the vehicle scales.

#### **D. Integration of Cost, Reliability, and Performance Models**

Once the ROSETTA models are completed for each of the vehicles required in the lunar mission mode, the vehicles must be integrated into a lunar architecture selection tool. To complete the lunar architecture DSM, the individual vehicle models must be included in an integrated framework to pass the vehicle mass, costs, and reliabilities between the elements of the architecture. ModelCenter is an integrated framework ideally set up to integrate multiple Excel based models and pass information between the models [20]. Each of the ROSETTA models were wrapped in ModelCenter wrappers and vehicle masses, costs, and reliabilities are then passed between the different ROSETTA models to complete the lunar architecture.

A separate inputs and cost accumulator module were also included in the integrated framework. The inputs module conditioned the vehicle level inputs so that the full lunar architecture is simulated. An example of this is that the Inputs page takes a user's selection of the lunar orbit rendezvous mission mode and sets the individual vehicles to perform the proper burns to complete the lunar orbit rendezvous. The resulting methodology is summarized in the flow chart presented as Figure 3.

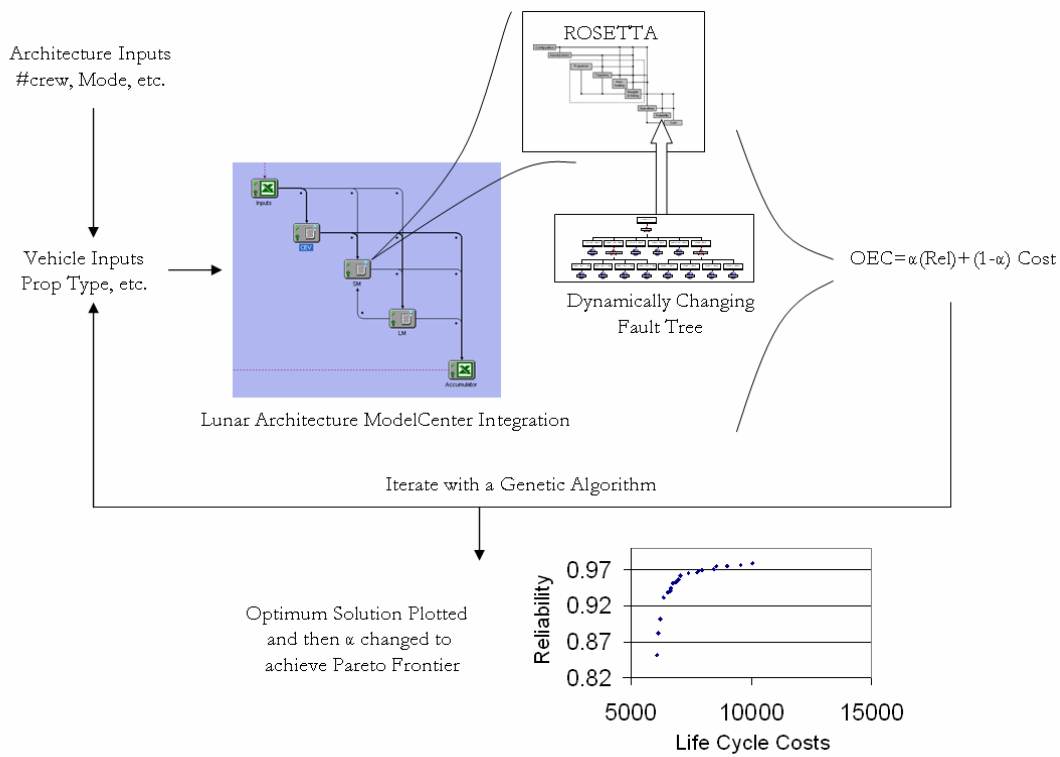


**Figure 3: Integrated Lunar Architecture Selection Tool.**

As this figure shows, the GA takes the place of the Monte Carlo analysis and an Overall Evaluation Criteria (OEC) is used as the objective function of the optimizer. This method is stochastic in that the initial population is randomly generated, but as a result of the higher objective function solution stay in the simulation longer, more points are evaluated around the Pareto frontier than a Monte Carlo analysis for a given number of simulations. The GA is solved for a given weighting ( $\alpha$ ) on the OEC. The OEC is given as equation 9.

$$OEC = \alpha \left( \frac{R}{R_{BL}} \right) + (1 - \alpha) \left( \frac{LCC_{BL}}{LCC} \right) \quad (9)$$

The baseline LCC and R are different for the different lunar modes that are optimized. Each baseline is either the baseline numbers computed for the Apollo mission modes. Each baseline was verified and then simulated using the generic lunar mission cost spreading. This method optimizes the Pareto frontier on an OEC constructed of loss of mission reliability and life cycle cost. This weighting ( $\alpha$ ) is then changed and the GA is rerun to find a second point on the Pareto frontier. The aforementioned procedure continues until enough points in the Pareto frontier are defined to adequately evaluate the Pareto frontier.

### III. Validation

To verify this design methodology and to validate the accuracy of the ROSETTA models, each of the mission modes under consideration was simulated and compared with the solutions obtained using the conventional conceptual design techniques. To baseline this methodology, the three Apollo modes that were under consideration in the 1960s (Earth Orbit Rendezvous, Lunar Orbit Rendezvous, and Lunar Direct Missions) were simulated and

compared with the solutions obtained in the Apollo Program. Once the procedure is verified, it was used to calculate the optimal Pareto frontiers for each of the mission modes.

To accomplish this simulation a complete ROSETTA model was created for each of the vehicles in the lunar architectures. These ROSETTA models were individually validated and then compiled into a lunar architecture using a ModelCenter integration environment. This ModelCenter based simulations will then be used to compute the performance, cost, reliability, and safety for each of the lunar mission modes. These results (performance, cost, and reliability) are then compared with the results from a conventional conceptual design process to validate the method and the results of each of the lunar architecture simulations.

Perhaps the most recognizable mission mode for lunar exploration is the Apollo Lunar Orbit Rendezvous mission mode. The LOR mission mode was originally championed by John Houbolt, a NASA Langley engineer [21]. This mission mode involved the use of a single Saturn V (C-5) launch vehicle to launch a three person Command Module (CM), a hypergolic pressure fed service module (SM), and a two person, two stage hypergolic pressure fed Lunar Module (LM). This mission mode is demonstrated in Figure 4.

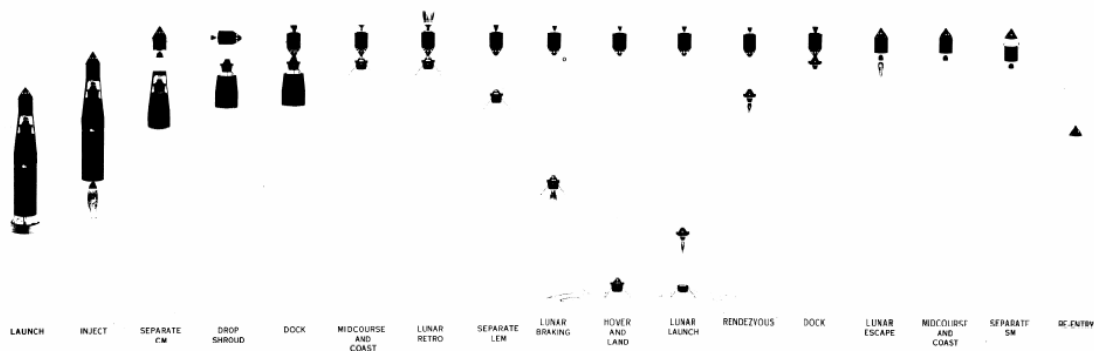


**Figure 4: Lunar Orbit Rendezvous Mission Mode [22].**

As this figure depicts, the Apollo LOR concept involves a single launch of a Saturn V launch vehicle. The Saturn V is a three stage launch vehicle consisting of an S-I C first stage, and S-II second stage and an S-IV B third stage. The three man crew resides in the Command Module (CM) during the ascent. The CM is an Aluminum capsule designed to carry the crew to the low lunar orbit and return them to the Earth. Once in Low Earth Orbit (LEO) the S-IV-B performs a burn (Trans Lunar Injection (TLI)) to propel the vehicle stack to the Moon. The Service Module (SM) enters the stack (Lunar Module (LM) and CM) into Low Lunar Orbit (LLO). The Lunar Module is designed to take two men (via a separate habitat) to the lunar surface from low lunar orbit. The third man remains in the CM for the duration of the lunar surface mission. The LM is a two stage vehicle that uses common propellants as the SM. The staging point for the LM is at the lunar surface. The Lunar Ascent Module then returns the two man lunar crew to LLO and rendezvous with the CM and the SM. The SM propels the CM to earth by performing the trans-earth injection (TEI) burn. The CM subsequently enters the Earth's atmosphere and descends via parachutes for a water touch down. A compilation of the design choices made in the Apollo LOR mission is given below as Table 4 and Table 5.

**Table 4: Propellant Choices for Apollo Lunar Orbit Rendezvous.**

<i>Vehicle</i>	<i>Propellants</i>	<i>Engine</i>	<i>Engine Number</i>
S-I-C	LOX/RP1	F-1 (Gas Generator)	5
S-II	LOX/LH2	J-2 (Gas Generator)	5
S-IV B	LOX/LH2	J-2 (Gas Generator)	1
SM	UDMH/N2O4	Pressure Fed	1
LM Descent	UDMH/N2O4	Pressure Fed	1
LM Ascent	UDMH/N2O4	Pressure Fed	1

**Table 5: Structure Choices for Apollo Lunar Orbit Rendezvous.**

<i>Structure</i>	<i>Main Tanks</i>	<i>Pressurant Tanks</i>	<i>Other Structure</i>
S-I-C	Al	Ti	Al
S-II	Al	Ti	Al
S-IV B	Al	Ti	Al
CM	NA	Al	Al
SM	Al	Ti	Al
LM Descent	Al	Ti	Al
LM Ascent	Al	Ti	Al

It is important to note that the Apollo LOR mission mode assumes the same engines for the second and third stages of the Saturn V. This is important because the DDT&E for this engine can be shared by both stages. The same is true for the LM descent engine and the SM engine. These engines used the same propellant and are approximately the same thrust levels so a cost benefit also occurs.

The Apollo LOR was simulated in ModelCenter using ROSETTA models. The simulation involved the creation of ROSETTA models for the Command Module, the Service Module, the Lunar Module, and the Saturn V. These ROSETTA modules were then wrapped in ModelCenter to integrate the performance characteristics of the mission mode. The Architecture Cost Model (ACM) was also integrated to compile the costs of the different vehicles can then calculate the total Life Cycle Costs (LCC) of the mission mode.

The Apollo LOR baseline was computed using this ROSETTA based simulation tool. The 83 design variables were set and the ROSETTA models were evaluated to close the Apollo LOR mission mode. The performance results were compared between the simulation results and the actual Apollo LOR vehicle weights [23]. The results are given as Table 6.

**Table 6: Comparison of Apollo Lunar Orbit Rendezvous Performance Results.**

	<i>Apollo Baseline</i>	<i>ROSETTA Models</i>	<i>% Diff</i>
CM	5,920 kg	6,020 kg	1.72%
SM	24,720 kg	24,920 kg	0.79%
LM	16,440 kg	16,180 kg	-1.54%
Stack	47,080 kg	47,120 kg	0.09%
S-I-C	2,279,000 kg	2,280,000 kg	0.04%
S-II	484,000 kg	477,200 kg	-1.40%
S-IV	122,700 kg	128,400 kg	4.61%
CES	4,160 kg	4,110 kg	-1.32%
On Pad	2,937,000 kg	2,936,000 kg	-0.01%

As this table shows, the mass results for the ROSETTA models are within 5% of the actual vehicle weights. The biggest discrepancy is on the Saturn IV-B stage. This large discrepancy may be due to the fact that any errors in the stack weight are compounded in the TEI stage since it must perform the large delta V (~10,000 ft/s) required for that burn. The entire stack weight is within 0.01% of the actual mass of the Saturn V vehicle at the pad. These mass estimations are very accurate and have to do with the fact that very few manned space vehicles have been built and the MERs used in the ROSETTA models have been based upon this limited vehicle set which includes the Apollo vehicles.

The mass estimates for the Apollo LOR mission mode are very accurate; and therefore, a mass-based cost comparison can be made between the Apollo architecture costs and the ROSETTA model calculated costs. As noted previously, these Cost Estimating Relationships (CERs) are bottoms-up subsystem based costing methods. These NAFCOM based CERs scale according to the mass of the subsystems and the complexity of the subsystem as compared with the baseline. The resulting simulation costs are then compared with the NAFCOM published cost

for the Apollo vehicles. The comparison of Design Development Testing & Evaluation (DDT&E) is given as Table 7 and the Theoretical First Unit (TFU) costs are given as Table 8.

**Table 7: Apollo Lunar Orbit Rendezvous Design Development Testing and Evaluation Cost Comparison.**

<i>\$M 2004</i>	<i>Apollo</i>	<i>ROSETTA Models</i>	<i>% Diff</i>
CSM	\$10,510 M	\$10,780 M	2.55%
LM	\$6,752 M	\$6,639 M	-1.67%
Saturn V	\$13,890 M	\$13,740 M	-1.03%
Total DDTE	\$31,140 M	\$31,160 M	0.04%

**Table 8: Apollo Lunar Orbit Rendezvous Theoretical First Unit Cost Comparison.**

<i>\$M 2004</i>	<i>Apollo</i>	<i>ROSETTA Models</i>	<i>% Diff</i>
CSM	\$294 M	\$309 M	5.10%
LM	\$651 M	\$733 M	12.60%
Saturn V	\$901 M	\$832 M	-7.71%
Total TFU	\$1,846 M	\$1,874 M	1.49%

As these tables show, the costs are very close for each of the vehicles in the Apollo LOR. DDT&E costs are within 3% for all of the elements of the architecture. The error associated with the TFU costs is slightly higher. The main difference is in the TFU of the LM. This higher cost of 12% results in a difference of \$82 million dollars. Even with this difference, the total TFU is only off by 1.49%, or \$8 million dollars, for the first vehicle. The ROSETTA calculated cost to first vehicle is \$33.03 Billion which is less than 0.1% off the actual cost to first vehicle of \$32.99 Billion.

The dynamically changing fault tree analysis incorporated in each ROSETTA model calculates the total vehicle reliability based upon the assumed subsystem reliabilities and the vehicle configurations. The reliability analysis was conducted for each of the ROSETTA models in the Apollo LOR, and the results were compared with those published in the Apollo Reliability and Quality Assurance Program Quarterly Status Report [24]. The resulting reliability comparisons are given in Table 9.

**Table 9: Apollo Lunar Orbit Rendezvous Loss of Mission Reliability Comparison.**

	<i>Apollo</i>	<i>ROSETTA Models</i>	<i>% Diff</i>
CSM	0.7662	0.7648	-0.19%
LM	0.8894	0.8918	0.27%
Stack	0.6815	0.6820	0.08%
Saturn V	0.7639	0.7690	0.66%
LOM	0.5206	0.5245	0.75%

As this table shows, the resulting Apollo LOR reliability calculations are within 1% of the actual calculated Apollo LOR reliabilities. This high level of accuracy is achieved because of the subsystem reliabilities are derived from the actual Apollo numbers. The total calculated LOM is 0.5245, or a loss of mission in every 2.10 flights. The demonstrated LOM of the Apollo LOR system is 1 loss in 7 flights or 0.87. For comparison purposes, the different lunar mode reliabilities will be based upon the calculated reliabilities and not the demonstrated reliabilities of the LOR.

The ROSETTA model accurately calculates the performance, cost, and reliability of the Apollo LOR mission mode. These ROSETTA models, combined in the ModelCenter environment, will then be used to find the Pareto frontiers of the ideal reliabilities for the varying budgets of the LOR program. This analysis was also conducted for the Apollo Direct and Apollo EOR mission modes. The errors are similar to that of Apollo LOR and are therefore not shown in this paper.

#### IV. Lunar Architecture Selection Using Pareto Frontiers

The optimization scheme outlined in section II is implemented into a lunar architecture selection tool to simulate the Apollo Lunar Orbit Rendezvous mission mode. The design variables above are optimized via a genetic algorithm to find the optimal OEC for a given weighting. This weighting on the OEC is then systematically changed from 100% reliability-centric to 100% cost-centric. Each optimized point is then plotted to produce a Pareto frontier of the Apollo LOR architecture. The optimized Pareto frontier for 10 different weightings of the OEC is given as Figure 5. The actual inputs chosen for by the genetic algorithm represented by the points on the Pareto frontier is given as Figure 6.

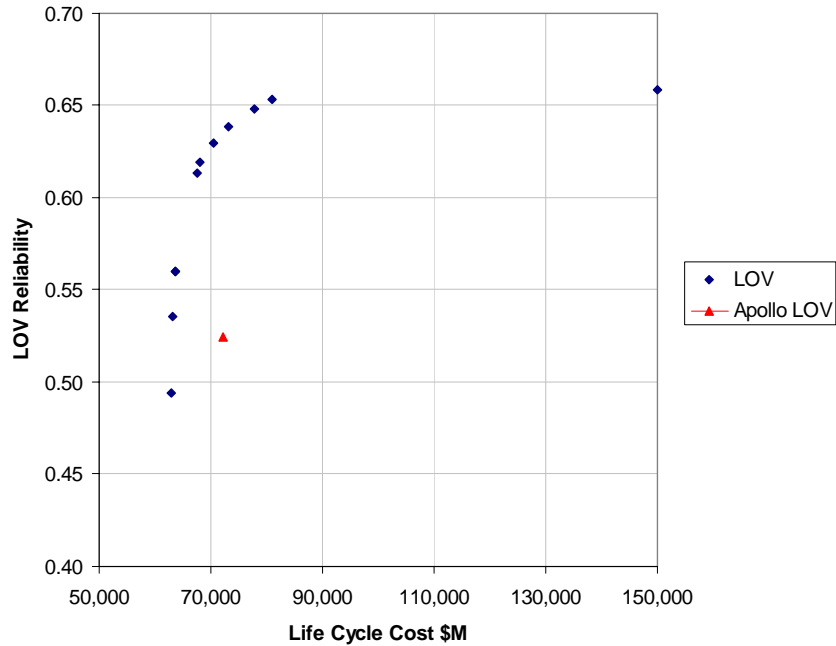


Figure 5: Pareto Frontier of the Apollo Lunar Orbit Rendezvous Architecture.

	Rel	90% Rel	80% Rel	70% Rel	60% Rel	50% Rel	40% Rel	30% Rel	20% Rel	10% Rel	Cost	Apollo	
CEV	Structure	Ti	Al										
	RCS	Hypergolic	Hypergolic	Hypergolic	Hypergolic	Hypergolic	Hypergolic	Hypergolic	Hypergolic	Hypergolic	Hypergolic	Hypergolic	
	Avionics Red	1	1	1	1	1	1	1	0	0	0	0	
	ECLSS Red	1	1	1	1	1	0	0	0	0	0	0	
	Parachute Red	1	0	0	0	0	0	0	0	0	0	0	
SM	Propellant Type	LOX/CH4	LOX/CH4	Hypergolic	LOX/CH4	LOX/CH4	LOX/CH4	LOX/LH2	LOX/LH2	LOX/LH2	LOX/LH2	LOX/LH2	Hypergolic
	Engine Type	Expander	Expander	Pressure	Expander	Pressure							
	Structure Type	Ti	Al	Al									
	Engine Red	1	1	1	0	0	0	0	0	0	0	0	0
	Pressurant Mat	Ti	Ti	Ti	Ti	Ti	Ti	Ti	Ti	Ti	Ti	Ti	Al
LM	Ascent Fuel Type	Hypergolic	Hypergolic	Hypergolic	Hypergolic	Hypergolic	Hypergolic	Hypergolic	Hypergolic	Hypergolic	Hypergolic	Hypergolic	Hypergolic
	Descent Fuel Type	LOX/CH4	LOX/CH4	LOX/CH4	LOX/CH4	LOX/CH4	LOX/CH4	LOX/CH4	Hypergolic	Hypergolic	Hypergolic	Hypergolic	Hypergolic
	T/W LS	2	2	2	2	2	2	2	2	2	2	2	2
	T/W LLO	2	2	2	2	2	2	2	2	2	2	2	2
	Engine Red Ascent	1	1	1	1	0	0	0	0	0	0	0	0
	Engine Red Descent	1	1	0	0	0	0	0	0	0	0	0	0
	AR Ascent	75	75	75	75	150	150	150	150	150	150	150	150
	AR Descent	75	75	150	150	150	139.2857143	150	128.5714286	128.5714286	128.5714286	139.2857143	75
	Ascent Engine Cycle Type	Pressure	Expander	Pressure									
	Descent Engine Cycle Type	Expander	Expander	Expander	Expander	Expander	Expander	Expander	Expander	Expander	Expander	Expander	Pressure
LV	Stage 1 Engine Type	Gas Gen	Gas Gen	Staged-Comb	Gas Gen								
	Stage 1 Propellant Type	LOX/RP1	LOX/RP1	LOX/RP1	LOX/RP1	LOX/RP1	LOX/RP1	LOX/RP1	LOX/RP1	LOX/RP1	LOX/RP1	LOX/RP1	LOX/RP1
	Stage 1 Structure Type	Ti	Al	Al									
	Stage 2 Engine Type	Gas Gen	Staged-Comb	Staged-Comb	Gas Gen	Gas Gen	Staged-Comb	Staged-Comb	Staged-Comb	Staged-Comb	Staged-Comb	Staged-Comb	Gas Gen
	Stage 2 Propellant Type	LOX/RP1	LOX/RP1	LOX/RP1	LOX/LH2	LOX/LH2	LOX/RP1	LOX/RP1	LOX/RP1	LOX/RP1	LOX/RP1	LOX/RP1	LOX/LH2
	Stage 2 Structure Type	Ti	Al-Li	Al	Al								
	Stage 3 Engine Type	Gas Gen	Staged-Comb	Staged-Comb	Gas Gen	Gas Gen	Staged-Comb	Staged-Comb	Staged-Comb	Staged-Comb	Staged-Comb	Staged-Comb	Gas Gen
	Stage 3 Propellant Type	LOX/RP1	LOX/RP1	LOX/RP1	LOX/LH2	LOX/LH2	LOX/RP1	LOX/RP1	LOX/RP1	LOX/RP1	LOX/RP1	LOX/RP1	LOX/LH2
	Stage 3 Structure Type	Ti	Al-Li	Al-Li	Al	Al							
	Stage 1 Engine Out	1	1	1	1	1	1	1	1	1	1	0	0
Stage 2 Engine Out	1	1	1	1	1	1	1	1	1	1	0	0	
Stage 3 Engine Out	1	1	1	1	1	1	0	0	0	0	0	0	

Figure 6: Summary of GA Produced Inputs for Apollo Lunar Orbit Rendezvous Architecture.

This Pareto frontier shows the expected dimensioning returns shape of increased reliability as a function of cost. The summary of the inputs shows how the different configuration choices are made as the weighting for the OEC changes. Some interesting observations can be made from the changing inputs driven by the GA and the weighting on the OEC. First, the redundancy changes dramatically as the weighting on the OEC changes. In the 100% reliability-centric optimization, redundancy exists on all 11 elements of the architecture. This is expected since the solution is independent of cost and therefore any increase in reliability (especially through redundancy) is chosen. This 100% reliability centric model utilizes mostly titanium structures in the vehicle designs. This is because titanium results in a lighter vehicle and with lower thrust engines, and therefore a higher reliability. Propellant types vary throughout the architecture vehicles, but LOX/CH<sub>4</sub> and the hypergolic propellants are most prevalent. Methane becomes an option because it offers higher performance (smaller engines with greater reliability) than hypergolic propellants, yet is more reliable than hydrogen due to the increased density of the fuel.

As the weighting increased towards 100% cost-centric, the propellant and structure types change as well as the redundancy in the system. The all cost optimization results in an all aluminum main structure with higher strength materials for the high pressure pressurant tanks. These structures are chosen because Al is the cheapest material per pound, while the higher strength materials are needed for the pressurant tanks due to the high weight (and cost) associated with the use of aluminum for those tanks.

It is interesting to look at the results of the changes in redundancy as the weighting on the OEC is changed from 0% reliability-centric to 100% reliability-centric. As expected, there are no redundant components in the 0% reliability-centric weighting. As the weighting increases to 10%, redundancy is added to the second stage of the Saturn launch vehicle. This is the first element of the architecture to gain redundancy. This is the case because of a balance between the reliability gained and the cost in mass and actual dollars of adding a redundant component. The second stage engine is added first because the engines on the second stage are generally lower reliability than that of the first stage engines (due to air start) and have a lower reliability than the third stage, due to the fact that 5 engines are operating instead of 1 engine on the third stage.

The second element to gain redundancy is the first stage of the Saturn launch vehicle. This occurs because of the fact that there are again 5 engines operating and the addition of a redundant engine adds significantly to the reliability of the system. This also occurs because there is very little mass penalty for adding a first stage engine because that extra weight is only carried by the first stage.

As the weighting is increased more component and subsystem redundancies are added as a compromise between weight, cost, and reliability. A general rule is that the lower reliability of the system the earlier a redundant component is going to be added. Unfortunately it is not that simple, since an extra pound on the CM does translates too many extra pounds on the launch vehicle due to the gear ratio of the architecture. This gear ratio simply states that an extra pound on the CM, must be pushed by the SM which adds several extra pounds, which must then be launched which adds pounds exponentially according to the rocket equation. This exponential relationship greatly affects the mass and therefore cost of the system. This gear ratio for the Apollo LOR components is demonstrated in Table 10.

**Table 10: Gear Ratio for Apollo Lunar Orbit Rendezvous Architecture Elements.**

	<i>CM</i> (+1000kg)	<i>SM</i> (+1000kg)	<i>LM</i> (+1000kg)	<i>S-IVB</i> (+1000kg)	<i>S-II</i> (+1000kg)	<i>S-I-C</i> (+1000kg)
CM	1,167 kg	0 kg	0 kg	0 kg	0 kg	0 kg
SM	1,697 kg	3,595 kg	3,614 kg	0 kg	0 kg	0 kg
LM	0 kg	0 kg	7,521 kg	0 kg	0 kg	0 kg
S-I-C	127,400 kg	125,100 kg	454,900 kg	34,780 kg	11,310 kg	4,312 kg
S-II	27,200 kg	26,700 kg	103,000 kg	7,427 kg	3,415 kg	0 kg
S-IVB	7,599 kg	7,460 kg	23,120 kg	3,075 kg	0 kg	0 kg
Total	165,000 kg	162,800 kg	592,200 kg	45,280 kg	14,730 kg	4,312 kg
GR	165	163	592	45	15	4

This table demonstrates the effect of 1000 kg of dry weight growth on a vehicle element and the resulting stack growth. The gear ratio is highest for the lunar module. This is because of the high  $\Delta V$  that must be performed by the stages as well as the fact that the LM is payload for both the SM and the Saturn V elements. Because the CM is not payload for the lunar module, but is for the SM and the Saturn lowers the gear ratio when compared to the LM.

The CM gear ratio is higher than that of the SM because of the fact that the CM is carried as payload of the CM. The gear ratio of the CM is not higher because of the fact that the CM has little onboard propellant, so the increase in dry weight has a small affect on the gross weight of the CM. The Saturn stages have increasing gear ratios as you increase the stage of the vehicle. As with the LM, this is because the uppers stages act as payload for the lower stages. This table shows that a pound growth on the LM has the greatest impact on the total vehicle stack for the Apollo LOR architecture. This directly impacts the order of increasing subsystem redundancy in the Apollo LOR architecture. A summary of the increase of redundant components as the weighting on the OEC becomes more reliability-centric is shown as Figure 7.

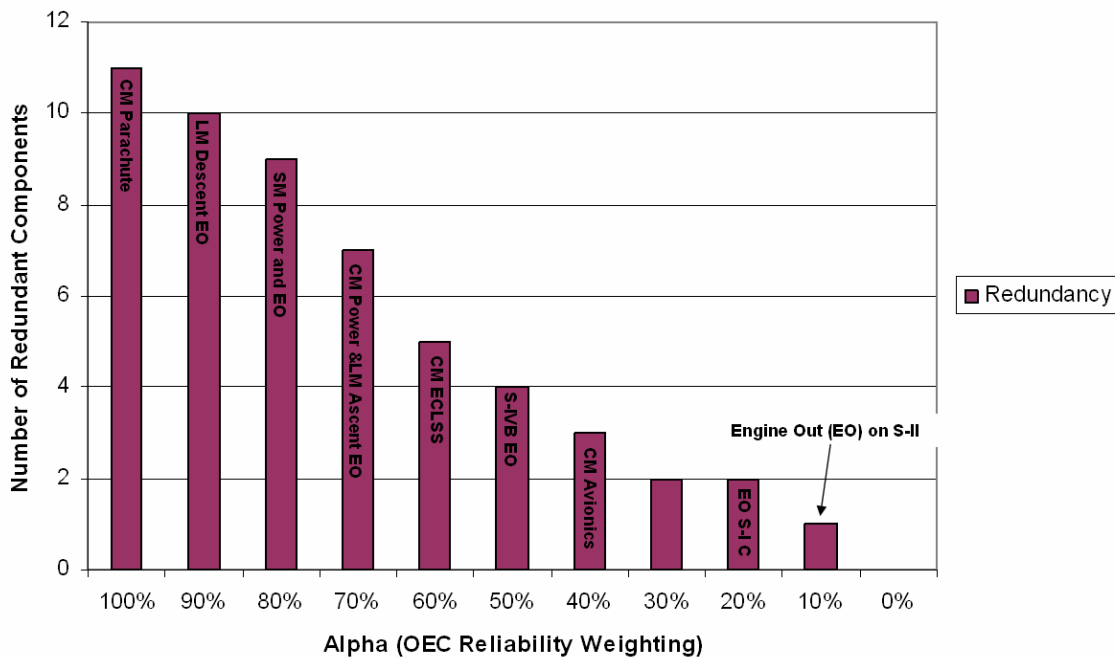


**Figure 7: Redundancy in the Apollo Lunar Orbit Rendezvous Pareto Frontier.**

As figure shows, the redundancy steadily increases to the maximum of eleven redundant components as the weighting on the reliability increases. The final redundant component added is the parachute redundancy. This is the last redundant component added because the descent system for the CM is generally considered a high reliability system and an extra parachute adds a significant weight to the top of the lunar architecture.

As noted in Figure 5, the optimal Pareto frontier is significantly higher reliability and lower cost than the baseline Apollo architecture. These optimal points are able to retrieve higher reliabilities and lower costs than the baseline Apollo because of the constraints placed on the Apollo project. The Apollo lunar mode decision was made under intense schedule pressure placed on it by the John F. Kennedy's decree that the Apollo program would send a man to the moon before the end of the decade. This schedule constraint is not modeled in this methodology and therefore pushes the Apollo LOR Pareto frontier optimal past the Apollo baseline. The schedule based design choices of hypergolic propellants and limited redundancy pushed the Apollo baseline off the optimal result. A comparison of the Apollo baseline to the optimal reliability Pareto point for the same Apollo cost, and the optimal cost point to the Apollo cost is given as Figure 8.

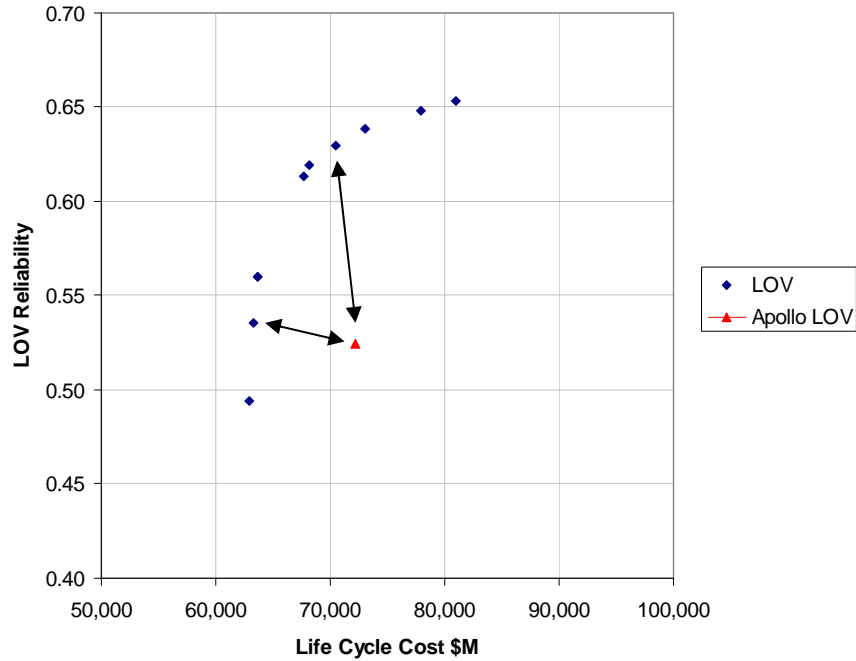


**Figure 8: Comparison of Apollo Baseline to Pareto Frontier Optimal Points.**

**Table 11: GA Input Differences Between Apollo Baseline and Pareto Frontier.**

		<i>Improved Reliability</i>	<i>Improved Cost</i>	<i>Apollo</i>
<b>CM</b>	Avionics Red	1	0	0
	ECLSS Red	1	0	0
	Power Red	1	0	0
<b>SM</b>	Propellant Type	LOX/CH4	LOX/LH2	Hypergolic
	Engine Type	Expander	Expander	Pressure
<b>LM</b>	Descent Fuel Type	LOX/CH4	Hypergolic	Hypergolic
	Engine Red Ascent	1	0	0
	Engine Red Descent	0	0	0
	AR Ascent	75	150	75
	AR Descent	150	128.5714286	75
	Ascent Engine Cycle Type	Expander	Expander	Pressure
<b>LV</b>	Descent Engine Cycle Type	Expander	Expander	Pressure
	Stage 1 Engine Type	Staged-Comb	Staged-Comb	Gas Gen
	Stage 1 Propellant Type	LOX/RP1	LOX/RP1	LOX/RP1
	Stage 1 Structure Type	Al	Al	Al
	Stage 2 Engine Type	Gas Gen	Staged-Comb	Gas Gen
	Stage 2 Propellant Type	LOX/LH2	LOX/RP1	LOX/LH2
	Stage 2 Structure Type	Al	Al	Al
	Stage 3 Engine Type	Gas Gen	Staged-Comb	Gas Gen
	Stage 3 Propellant Type	LOX/LH2	LOX/RP1	LOX/LH2
	Stage 3 Structure Type	Al	Al	Al
	Stage 1 Engine Out	1	1	0
	Stage 2 Engine Out	1	1	0
	Stage 3 Engine Out	1	0	0

Figure 8 demonstrates that a cost improvement of almost \$9 B FY2004 dollars can be saved over the 20 year life of the program, while keeping the same reliability as the baseline Apollo architecture. If the life cycle cost was kept constant, an increase in LOM reliability of 0.1137 can be obtained.

As with reliability, LOC safety Pareto frontier can also be created. The Pareto frontier is very similar to the curve calculated for LOM since the LOM and LOC are similar for a given architecture. To calculate this Pareto frontier, the LOC safety numbers were calculated for the given LOM Pareto frontier points. The simulation could be reoptimized for LOC, but since the dependencies on LOM and LOC are interrelated and the Pareto frontier is of similar shape, the LOC of the optimized LOM points was used for the Pareto frontier. The Pareto frontier for LOC is included as Figure 9.

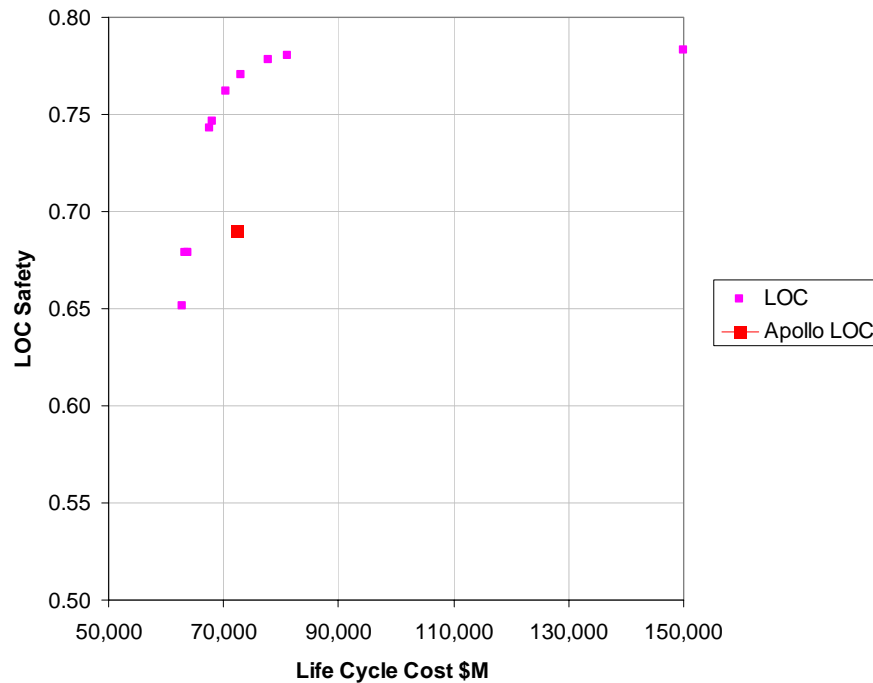


**Figure 9: LOC Pareto Frontier for Apollo Lunar Orbit Rendezvous.**

As this figure shows an increase in LOC safety of 0.0803 can be achieved with the same cost as the baseline Apollo architecture. A summary of the savings in reliability and cost are summarized in Table 12.

**Table 12: Differences Pareto Frontiers and Baselines.**

<i>\$M</i>	<i>LOR</i>	<i>%Diff</i>
LCC	\$8,958	12%
LOM	0.11	21%
LOC	0.08	12%

As this tables shows, the cost savings to achieve the same reliability as the baseline is at least \$8.9 B FY2004. Cost savings of up to 12% over the Apollo baselines can be achieved with the application of this methodology. The reliability gains can be 21% for reliability and 12% for safety while keeping approximately the same cost as the baseline. This same methodology can be completed for the Apollo EOR, Apollo Direct, and Exploration System Architecture Study mission modes resulting in similar savings in both cost and reliability by using the optimal Pareto frontier in the architecture configuration selection.

## V. Conclusions

The goal of this research was to develop a lunar architecture selection tool that would revolutionize the design process by presenting the decision maker with the ideal cost and reliability solutions. This goal was accomplished through the adaptation of the current design process to include fast acting parametric ROSETTA models with dynamically changing cost and reliability analyses. These new parametric tools were then combined in an integrated framework to evaluate the optimal Pareto frontiers for a given lunar mode. The developed Pareto frontiers present the optimal cost and reliability solutions to the decision maker without bogging down the decision maker with the performance details of the architecture elements.

In conclusion, this method can accurately and quickly evaluate lunar architectures. The dynamic calculations of performance, cost, and reliability allow the decision maker to be presented with information about the cost and reliability of multiple optimal solutions. These optimal solutions, presented as a Pareto frontier, can be used to select the best lunar architecture and mission mode for any design budget. The resulting solutions can save between \$9 B for the same reliability when compared over a 32 flight lunar campaign. For the same cost, this method can increase the reliability of 21%. This research can also be extended to find the ideal Pareto frontier for other lunar modes such as the Apollo Direct, Apollo Earth Orbit Rendezvous, and the Exploration System Architecture Study.

## Acknowledgments

The authors would like to thank the members of the Space Systems Design Lab at the Georgia Institute of Technology.

## References

- 1 Loch, C. H., M. T. Pich, C. Terwiesch and M. Urbchat: Selecting R&D Projects at BMW: A Case Study of Adopting Mathematical Programming Models, IEEE Transactions on Engineering Management 48 (1), 2001, 70 - 80.
- 2 Schmidt, RL, JR Freeland. 1992. Recent progress in modeling R&D project-selection processes. IEEE Trans. Eng. Management 39(3) 239-246
- 3 Beaujon, G. J., S. P. Marin., G. C. McDonald. 2001. Balancing and optimizing a portfolio of R&D projects. Naval Logist. Quart. 48(1) 18-40.
- 4 Marcus, L., Olds, J. R., et. al., "Technology Assessment for Manned Mars Exploration Using a ROSETTA Model of a Bimodal Nuclear Thermal Rocket (BNTR)," AIAA Space 2001 Conference and Exposition, Albuquerque, NM, August 28-30, 2001.
- 5 Rocket Engine Design Tool for Optimal Performance (REDTOP), Software Package, ver 1.3, Spaceworks Engineering Inc., Atlanta, GA, 2003.
- 6 Krevor, Z. Space Systems Design Laboratory, Georgia Institute of Technology (2006) Unpublished raw data.
- 7 Powell, R.W., et. al., "Program to Optimize Simulated Trajectories (POST) Utilization Manual, Volume II, Version 5.2," NASA Langley Research Center, Hampton, VA; Martin Marietta Corporation, Denver, CO., October 1997.
- 8 Thompson, R. Space Systems Design Laboratory, Georgia Institute of Technology (2006) Unpublished raw data.
- 9 Rohrschneider, R., "Development of a Mass Estimating Relationship Database for Launch Vehicle Conceptual Design," AE8900 Special Project, School of Aerospace Engineering, Georgia Institute of Technology, April 26, 2002.
- 10 Willoughby, L. "A Semi-empirical Method for Propellant Tank Weight Estimation," 27th Annual Conference of the Society of Aeronautical Weight Engineers, Inc. New Orleans, LA 1968.
- 11 Humble, R., Henry, G. , and Larson, W. *Space Propulsion Analysis and Design*. McGraw-Hill Companies New York, NY. 1995.
- 12 Mosleh, A. et al. "Procedure for Treating Common-Cause Failures in Safety and Reliability Studies," U.S. Nuclear Regulatory Commission, NUREG/CR-4780, Vol. I and II, Washington, DC. 1988.
- 13 Fleming, K. N., Molesh, A. "Common-Cause Data Analysis and Implications in System Modeling," Procedures Int'l Topical Meeting on Probabilistic Safety Methods and Applications, Feb 1985. Vol 1.

- 14 Tang, Zhihua, Dugan, Joanne. "An Integrated Method for Incorporating Common Cause Failures in System Analysis," *Annual Reliability and Maintainability Symposium 2004 Proceedings*, LA, January 2004.
- 15 Modarres, M. *What Every Engineer Should Know About Reliability and Risk Analysis*. Marcel Dekker, Inc. New York, NY 1993.
- 16 Huang, Z. Fint, J., Kuck, F. "Key Reliability Drivers of Liquid Propulsion Engines and A Reliability Model for Sensitivity Analysis." 41st AIAA/ASME/SAE/ASEE Joint Propulsion Conference. Tucson, AZ. July 2005.
- 17 Relex Reliability Suite, Software Package, ver 2.2, Relex Software Corporation, Greensburg, PA, 2004.
- 18 NASA Air Force Cost Model, Software Package, ver. 2004, SAIC, Huntsville, AL, 2004.
- 19 SpaceshipOne, the Ansari X Prize and the Material of the Civilian Space Race. 3 May 2005<<http://www.tms.org/pubs/journals/JOM/0411/Byko-0411.html>>
- 20 ModelCenter, Software Package, ver 6.1.1, Phoenix Integration Inc., Philadelphia, PA, 2007.
- 21 Logsdon, J. M., "Selecting the Way to the Moon: The Choice of Lunar Orbital Rendezvous Mode," *Aerospace Historian*, Vol. 18, Summer 1971, pp. 63-71.
- 22 Reeves, D., Scher, M., Wilhite, A., Stanley, D., "The Apollo Lunar Orbit Rendezvous Architecture Decision Revisited," 41st AIAA/ASME/SAE/ASEE Joint Propulsion Conference and Exhibit, Tucson, AZ, July, 2005.
- 23 NASA Technical Document, "Mass Estimating and Forecasting for Aerospace Vehicles Based on Historical Data JSC-26098," Houston, TX. November, 1994.
- 24 NASA Technical Document, "Apollo Reliability and Quality Assurance Program Quarterly Status Report," Washington D.C., October 8, 1965.